Published in final edited form as:
Ann Biomed Eng. 2014 June ; 42(6): 1148–1157. doi:10.1007/s10439-014-0992-x.

Role of the Basement Membrane in Regulation of Cardiac Electrical Properties

Huaxiao Yang[1], **Thomas K. Borg**[2], **Zhonghai Wang**[1], **Zhen Ma**[3], and **Bruce Z. Gao**[1]

[1]Department of Bioengineering, Clemson University, Clemson, SC, USA

[2]Department of Regenerative Medicine, Medical University of South Carolina, Charleston, SC, USA

[3]Department of Bioengineering, University of California, Berkeley, CA, USA

Abstract

In the heart muscle, each adult cardiomyocyte is enclosed by a basement membrane (BM). This innermost extracellular matrix is a layered assembly of laminin, collagen IV, glycoproteins, and proteoglycans. In this study, the role of the BM network in regulation of the electrical properties of neonatal cardiomyocytes (NCMs) cultured on an aligned collagen I gel was investigated using a multielectrode array (MEA). A laminin antibody was added to the culture medium for 48–120 h to conjugate newly secreted laminin. Then, morphology of the NCMs on an MEA was monitored using a phase contrast microscope, and the BM network that was immunocytostained for laminin was imaged using a fluorescence microscope. When the BM laminin was absent in this culture model, dramatic changes in NCM morphology were observed. Simultaneously, the MEA-recorded cardiac field potential showed changes compared to that from the control groups: The period of contraction shortened to 1/2 of that from the control groups, and the waveform of the calcium influx shifted from a flat plateau to a peak-like waveform, indicating that the electrical properties of the NCMs were closely related to the components and distribution of the BM network.

Keywords

Basement membrane; Cardiomyocyte; Electrophysiology; Multielectrode array

INTRODUCTION

The basement membrane (BM) is a highly organized network of extracellular matrix (ECM) proteins that is closely associated with various types of cells, such as endothelial cells,[15] podocytes,[27] aortic smooth muscle cells,[33] Schwann cells,[25] and cardiomyocytes.[23] These proteins include laminins, type IV collagens, entactins, perlecan, and chondroitin sulfate

Address correspondence to Bruce Z. Gao, Department of Bioengineering, Clemson University, Clemson, SC, USA. zgao@clemson.edu.

ELECTRONIC SUPPLEMENTARY MATERIAL
The online version of this article (doi:10.1007/s10439-014-0992-x) contains supplementary material, which is available to authorized users.

proteoglycans.[9,37] Around each adult cardiomyocyte (ACM) in the heart, the BM forms a dense network; its thickness, based on observation under a transmission electron microscopy is 80 nm.[19]

For some organs and tissues, the physiological functions of the BM are known. In the kidney, the glomerular BM (GBM) is instrumental in glomerulogenesis: Without the GBM, a glomerular cell is unable to maintain its position, which leads to a disorganized glomerulus.[26] In the circulatory system, blood-vessel maturation requires the presence of laminin 8, a BM component.[15] The BM in skeletal muscle contributes to differentiation of the myotube and is crucial in development of the neuromuscular junction.[28] In the heart muscle, the BM is influential in sarcomeric formation and remodeling because of its interaction with integrins, which serve as receptors on the plasma membrane and orchestrate multiple myocardial functions, including organogenesis.[30] The BM has a key role in regulation of electrophysiology: Anionic sites composed of glycosaminoglycans, such as heparan sulfate, on the GBM regulate the negatively charged membrane potential, which is closely related to congenital nephrosis and albuminuria.[13,34]

Early studies of cardiac-cell culture in the 1970s and 1980s[12,19–21] showed that (1) the BM is capable of binding calcium ions and (2) removal of the BM causes an increased calcium-exchange rate. Two mechanisms of calcium exchange and storage that are involved in the excitation–contraction coupling of cardiac cells are (1) the calcium-induced calcium release mechanism supported by the sarcoplasmic reticulum[2] and (2) the calcium entry-release coupling mechanism supported by the surface membrane of transverse tubules (*t* tubules) distributed at *Z* lines.[6] These two mechanisms cooperatively regulate cardiomyocyte (CM) electrophysiology through control of calcium flux. The discovery that the BM laminin is capable of binding calcium outside the cellular plasma and buffering calcium influx[12,19] suggests that the BM may provide a third mechanism of calcium control. However, direct observation of the BM's role in the regulation of cardiac-cell electrical properties has not been reported.

Multielectrode arrays (MEAs) have the advantage of long-term, real-time recording of the electrical activities of cardiac cells at multiple sites in a live cell culture[8,24]; this provides a novel technique for study of the BM's electrophysiological role. In this paper, we report MEA results obtained from freshly isolated 3-day neonatal cardiomyocytes (NCMs) cultured on an aligned collagen I gel (ACG). The cultures were anti-laminin treated for 5 days to block the binding ability of newly secreted laminin and thus interfere with its polymerization. The achieved BM-deposition regulation was monitored under a phase-contrast microscope and through fluorescence imaging after immunocytostaining at Day 5. Simultaneously, the electrical properties of the treated NCMs were compared to untreated controls through MEA recording.

MATERIALS AND METHODS

Cell Harvest and Culture

Sprague–Dawley (SD) neonatal rats (Day 3) and adult rats (1 month) were euthanized according to a procedure approved by the Clemson University Institutional Animal Care and

Use Committee (Protocol number AUP2013-035). The procedure conforms to the Guide for the Care and Use of Laboratory Animals published by the US National Institutes of Health (NIH Publication, 8th Edition, 2011). The methods of euthanasia for neonatal animals are consistent with the recommendations of the Panel on Euthanasia of the American Veterinary Medical Association.

NCMs were isolated and collected from 3-day-old SD rats using the 2-day protocol we previously reported.[24] In brief, ten neonatal rats were dissected, and the ventricular portion of each heart was collected and minced in Moscona's Saline. The tissue was transferred to 50 mL Dulbecco's Phosphate Buffered Saline (DPBS) with 4 mg trypsin and 50 mg neutral protease and stored in a 4°C refrigerator overnight. The next day, the tissue was transferred into 50 mL Kreb's Ringers Bicarbonate Buffer (KRB) with 10 mg collagenase type I and 30 mg collagenase type II and then shaken in a water bath at 50 rpm for 45–60 min. The cell suspension was washed twice using cardiomyocyte culture medium (high glucose Dulbecco's Modified Eagle's Medium (DMEM) supplemented with 10% fetal bovine serum and 1% penicillin strep tomycin) to remove the enzyme residue. The isolated cells were transferred into a 150 cm^2 flask for a cell-adhesive assay to remove the cardiac fibroblasts. After 2 h, the unattached CMs were collected. Our immunocytostaining data and data from other groups that used the same CM purification procedure have demonstrated that 95% CM purification can be achieved.

NCMs Alignment on the ACG

First, the method of ACG coating was modified based on the literature[32] and is briefly described as follows: Type I collagen gel was prepared by mixing rat type I collagen solution (3.1 mg mL^{-1}, Advanced Biomatrix, Ltd., USA) with HEPES solution (0.1 M, pH = 9.0) at a ratio of 3:7 on an ice bath without intensive pipetting. On a cleaned, inclined 22 × 22 mm glass coverslip, one droplet (1 mL) pre-gel solution was dropped near an edge. After 30 s, during which the collagen fibers in the drop of solution settled on the surface, the solution was sucked up, leaving a very thin layer of collagen pre-gel on the glass. This layer of collagen pre-gel was then slowly guided by a cell scraper to form a unidirectional flow towards the opposite edge, wetting a strip of the cover glass surface. The same procedure was repeated strip by strip to coat a wide area. After being coated, the coverslip was incubated in a cell-culture incubator for at least 1 h. After incubation, the surface of the coverslip was rinsed with a PBS buffer. Finally, 1 mL freshly isolated NCMs (1×10^6/mL) were seeded onto the ACG-coated coverslip, which was then cultured in a standard cell-culture incubator (37 °C and 5% CO_2).

The ventricle of the heart from a one-month-old adult SD rat was used to prepare ventricular tissue slides with microtome-cyrostat sectioning. All tissues were frozen at –20 °C in tissue-freezing medium (Tissue-Tek OCT compound, Sakura Finetechnical Co., Ltd, Japan). Immediately after being frozen, the tissues were cut transversely (perpendicular to the interventricular septum) to produce 20 μm tissue slides using a cryostat (Leica CM1950, Wetzlar, Germany).

In vitro Culture of NCMs on MEA Chips

With the same method as on the coverslip, ACG was coated on the surface of an MEA chip, then 1 mL freshly isolated NCMs (1×10^6/mL) were seeded onto it, and it was then cultured in a standard cell-culture incubator (37 °C and 5% CO_2).

MEA Measurement of NCM Electrical Properties

The MEA chip (Fig. 1) contains 8 × 8 (200 μm apart) indium tin oxide (ITO) electrodes (30 μm in diameter) without TiN coating. Three groups of MEA chips were prepared: The anti-laminin group was created by adding rabbit-anti-rat IgG anti-laminin (laminin α1 (LAMA1), 1 mg mL^{-1}, 1:100, Abcam Inc., USA) to the culture medium to bind the newly secreted laminin at time points 24, 48, 72, and 96 h so as to interfere with its polymerization; the control group was created without antibodies; the IgG control group was created by adding rabbit-anti-rat IgG anti-CD105 to the culture medium at time points 24, 48, 72, and 96 h. The electrical properties of the NCMs from the three groups were measured by mounting MEA chips in the holder of an acquisition system (MultiChannel System Inc. Germany) at time points 48, 72, 96, and 120 h in a cell culture incubator at 37 °C and 95% humidity. MCS Rack V3.5.5 data-acquisition software was used with an A/D conversion set at a 50 kHz sampling rate. The raw signals from all electrodes (only 60 among the 64 electrodes were effective because the 4 corner electrodes were not wired by the manufacturer; these were discarded) were simultaneously recorded. The interval period of two adjacent peaks and the duration of each peak were measured based on the electrogram recorded at each electrode. The results were averaged from 12 electrodes.

IMMUNOCYTOSTAINING OF NCMS

BM Laminin

NCMs cultured on ACG-coated coverslips for 120 h were fixed with 4% paraformaldehyde (pH 7.4) solution for 15 min at room temperature (RT). Then they were blocked with blocking solution (4% (v/v) goat serum and 1% (v/v) BSA in PBS solution) for 30 min at RT. After blocking, they were washed once with PBS and incubated with 1 mL rabbit-anti-rat laminin PBS solution (1:300, Abcam Inc., USA) overnight at 4 °C. This procedure was followed by washing with PBS three times, each for 10 min, and incubation with 1 mL FITC-conjugated IgG goat-anti-rabbit PBS solution (1:200, Life Technologies, USA) for 1.5 h at RT in a dark room. They were then washed with PBS three more times; finally, the samples were covered with ProLong© antifade kit mounting medium (Life Technologies, USA) for fluorescence imaging later.

Double Staining of BM Laminin and Sarcomeric α-Actinin

After NCMs cultured on ACG for 192 h with BM laminin were stained, the cells were incubated with 1 mL mouse-anti-rat sarcomeric α-actinin PBS solution (1:500, Sigma, USA) overnight at 4 °C and then incubated with 1 mL TRITC conjugated IgG goat-anti-mouse PBS solution (1:200, Life Technologies, USA) for 1.5 h at RT in a dark room and washed with PBS 3 times, 5 min each. Finally, the sample was covered with ProLong© antifade kit mounting medium with DAPI (Life Technologies, USA) for fluorescence imaging later.

Double Staining of BM Laminin and F-actin

After NCMs cultured on ACG for 192 h with BM laminin were stained, the cells were incubated with Alexa Fluor® 594-conjugated phalloidin (1:100, Life Technologies, USA) for 1 h to stain *F*-actin, and then washed with PBS 3 × 5 min. Finally, the sample was covered with ProLong© antifade kit mounting medium with DAPI (Life Technologies, USA) for fluorescence imaging later.

Staining of Nucleus in the Ventricular Section

The ventricular section, after being fixed with 4% paraformaldehyde (pH 7.4) and treated with 1% Triton X-100, was incubated with 4′,6-Diamidino-2-phenylindole dihydrochloride (DAPI) solution (3 μM, Life Technologies, USA) for 1 h at RT to label the nucleus, then washed with PBS 3 × 5 min. Finally, the sample was covered with ProLong© antifade kit mounting medium (Life Technologies, USA) for fluorescence imaging later.

Imaging Immnuocytostained NCM Cultured on an MEA

The morphologies of the ACG coated on the coverslip and the NCMs cultured on 1) ACG-coated coverslip at 24 and 48 h and 2) MEA chips at 24, 48, 72, 96, and 120 h were imaged with the Zeiss Axiovert 200 M. ACG morphology was imaged by a scanning electron microscope (SEM, Hitachi 4800, Japan) after a series of ethanol dehydration and platinum sputtering, and the averaged diameter and length of the collagen fibrils were evaluated by the ImageJ (NIH, USA) based on 10 SEM images. The immunocytostained laminin, sarcomeric α-actinin, and *F*-actin were imaged with a fluorescence (Zeiss Axiovert 200 M) or confocal microscope (Nikon Eclipse Ti) for multichannel fluorescence-image acquisition. The nucleus pattern of the ventricular section was also imaged by the confocal microscope (Nikon Eclipse Ti) in the blue channel.

Cardiac Fibroblast to NCM Ratio

The cardiac fibroblast (CF)-to-NCM ratio cultured on an ACG-coated coverslip from Days 1-to-5 was evaluated based on the following equation:

$$x\,(CF \quad to \quad NCM \quad ratio) = \frac{\text{number of} \quad CF}{\text{number of} \quad CF + \text{number of} \quad NCM}$$

The number of NCMs was obtained from the sarcomeric α-actinin immunocytostaining images, and the number of CFs was obtained by counting the number of nuclei that were stained by DAPI and were not colocalized with the sarcomeric α-actinin.

Evaluation of Cardiac-Muscle Fiber-Like Structure

The cardiac muscle fiber-like structure that formed on ACG was evaluated by measuring the angle θ of the major axis of each nucleus against the orientation of the edge of the cardiac muscle fiber-like structure and a cardiac muscle tissue section by ImageJ (NIH, USA), shown in Fig. 2c:c1. Then the distribution of angles in the cardiac muscle fiber-like structure and cardiac-muscle tissue section groups was compared using histograms; the number of nuclei measured was 50–60 in each group.

Statistical Analysis

All data are presented as mean ± SD. Two groups of variables were compared using Student's *t* test. A value of $p < 0.05$ was considered significant.

RESULTS

NCM Culture on ACG

The ACG coating was achieved through aligning collagen fibrils that were evenly coated along the direction of scraping on the glass coverslip as shown in Figs. 2a:a1 and 2a:a2 with visualized collagen fibrils. The averaged diameter of the collagen fibrils was approximately 0.1 μm, and the length was longer than 40 μm based on the SEM images in Fig. 2a:a2. After freshly isolated NCMs were seeded on the ACG coating, they gradually polarized along the orientation of the collagen fibrils and grew into a rod-like morphology after being cultured for 24 and 48 h (Figs. 2a:a3, 2a:a4). After 192 h of myofibrillogenesis and remolding, a cardiac muscle fiber-like structure was formed. The confocal images of immunocytostained sarcomeric α-actinin, laminin, *F*-actin, and nuclei in Fig. 2b show ordered striated *Z*-lines (sarcomeric α-actinin). The thin filaments (*F*-actin)[22] oriented along the axis of the formed cardiac muscle fiber, which was tightly enclosed by a continuous BM laminin. Moreover, the alignment of the formed cardiac muscle fiber had nearly the same distribution as the cardiac muscle tissue revealed in Fig. 2c:c2, with the *p* value of $0.24 > 0.1$, suggesting that there was no significant difference between the two groups.

NCM Morphology on MEA chips

The NCMs in all three groups grew into a rod-like morphology with no obvious differences between groups; a large number of NCMs oriented in parallel (Figs. 3a, 3b, 3C, and 3d) at 24 and 48 h. As culture time increased from 72 to 120 h, NCMs in the anti-laminin group showed few phenotypic changes (Figs. 3f, 3h, and 3j). NCMs in the control group spontaneously aggregated into numerous clones, which were gradually enclosed by cardiac fibroblasts (Figs. 3e, 3g, and 3i). The zoom-out view of the NCMs in the two groups at 120 h (Figs. 3k, 3l) better demonstrates the morphological difference between the two groups. The IgG control group was morphologically similar to that of the control group (not presented herein). In addition, the proliferation of CFs from Day 1-to-Day 5, was unaffected by the treatment of anti-laminin (Fig. SI1).

BM Distribution on MEA Chips

The BM network around the NCMs cultured on the MEA chip was examined by laminin staining. Figure 4 demonstrates different distributions of laminin (green) in the culture of control and anti-laminin groups at 120 h: In the control, laminin mainly deposited around aggregated NCM clones (Fig. 4a) with dense intensity of fluorescence (Fig. 4c). In the anti-laminin group, laminin appeared as evenly distributed dots (Fig. 4d) without obvious aggregation (Fig. 4b).

Electrical-Property Changes of Anti-laminin Treated NCMs

NCMs were cultured on MEA chips coated with ACG, and the field potentials were measured from Day 2-to-Day 5. The development of the BM network was regulated by addition of an anti-laminin antibody to conjugate newly secreted BM laminin. To rule out nonspecific effects of IgG antibody, CD105 IgG antibody was chosen as the IgG control. With *in situ* tracing of the field-potential variations of NCMs from Day 2-to-Day 5 by the MEA chip, the most obvious change after addition of laminin antibody was that the period of NCM contraction in the control and the IgG control shortened from 0.25 s to 0.14 s on Days 3 and 4, shown in Fig. 5. Figure 6a shows that the waveforms of the field potential are identical for the control and IgG control groups with a flat plateau, while the field potential waveform for the anti-laminin group has a peak-like pattern. The duration of the field potential waveforms for both the plateau pattern and the peak pattern were measured; their summary showed significantly shortened duration of the calcium flux of the anti-laminin group compared to the controls (Fig. 6b). In addition, the interval periods of two peaks and durations of plateau of field potential are summarized in the Table 1.

DISCUSSION

The BM, an 80 nm thick inner layer of the ECM, serves as a layer of supportive material for the cells it encloses.[3,16,19] In cardiac muscle the BM network, dependent on its glycoprotein-based chemical properties, has a unique role in regulation of cardiac physiological functions.[11,19] In our study, we studied BM function using an *in vivo*-like cardiomyocyte-culture model on an ACG-coated MEA, and compared it to the other methods of cardiomyocyte alignment, such as microcontact printing and microabrasion,[4,7] the ACG coating on the MEA showed no damage to the glass surface and ITO electrodes. Laminin staining increases with time in culture, indicating that this BM component was being deposited as the CMs adapted to culture conditions. With these laminin-increase data as control, the anti-laminin (LAMA α1) experiments were conducted: LAMA α1 was added to the culture at intervals of 24 h starting from 24 h (Day 1) to 96 h (Day 4). The results demonstrated that the increase in basement membrane staining was not observed (Fig. 4d). Apparently the anti-laminin interfered with the assembly of the newly secreted laminin. It is generally accepted that LAMA α1 interferes with newly secreted laminin by attaching on the α1 chain, which is responsible for the self-assembly of laminin molecules to form a network.[13,15] However, we did not confirm this biochemically. The initial ACG coating characterized by those aligned collagen fibrils on the coverslip stimulated myofibrillogenesis in the NCMs, which assumed a 3D, rod-like morphology that mimicked the shape of an *in vivo* cardiomyocyte, shown in Fig. 2a. After 192 h of culture on ACG, the formed cardiac muscle fiber-like structure reflected the intensive interaction between NCMs and CFs with the confinement of ACG,[39] showing that the ACG coating was an ideal *in vitro* culture mode to mimic the *in vivo* structure of cardiac muscle fibers: The cardiomyocytes on the ACG expressed a rod-like shape, thus giving the BM formed around them an *in vivo*-like structure (Figs. 2b:b3, 2b:b7). Consequently the function, particularly the electrophysiological function, of the BM obtained in this *in vitro* model should be relevant *in vivo*.[32] With prolonged culture at 96 and 120 h, the morphologies of the NCMs in the control group changed dramatically into aggregated clones (Figs. 3e, 3g, 3i and 3k). This

is typical in an NCM culture in which CF proliferation is not prevented,[17] and secretion of growth factors by the CFs is the suspected cause.[1,39] Our data demonstrated that removal of the laminin component from the BM effectively delayed the aggregation of NCMs and maintained their alignment (Figs. 3e, 3g, 3i, 3k, and 3f, 3h, 3j, 3l), and that this was not caused by the decreased proliferation of CFs (Fig. SI1). Since the BM is known to be involved in binding and regulating bFGF,[14] TGF-β,[29] and other growth factors,[35] our laminin-removal data suggest that the BM network may have particular roles in regulation of growth factor-mediated signal transfer from fibroblasts to CMs.

In addition to the morphological difference between the anti-laminin and control groups, there were two major differences in electrical properties reflected by the field potential between the two groups—higher frequency of contraction and shorter field potential duration of the plateau (Figs. 5, 6a). The shape and the field potential duration of the plateau (and thus the frequency of contraction) are primarily affected by calcium influx from extracellular spaces.[5,11] The BM network is known to be capable of binding Ca^{2+} and plays a crucial role in calcium transmembrane exchange in the mammalian heart ventricle.[12,18,19,31] The BM laminin may be involved in the BM's Ca^{2+} binding and thus its regulation of the Ca^{2+} influx because (1) Ca^{2+} binding sites can be negatively charged protein polysaccharides,[12] and (2) it has been found that the assembly of laminin monomers into a polymer is dependent on calcium activation and binding.[37,38] Work by the Wang group showed decreased time of peak contraction and relaxation in cardiomyocytes isolated from laminin α4 chain-deficient mice in comparison with those from normal mice. The literature contains no comprehensive explanation of this phenomenon.[36]

The role of laminin in the basement membrane remains speculative. However, based on the above discussion, we argue that BM laminin is a major factor in the BM's Ca^{2+}-influx regulation. Consequently, both our data and Wang's observation can be explained: The peak-like waveform in the anti-laminin group in comparison with the flat plateau in the control groups was caused by the removal of the BM laminin. This removal was confirmed by immunocytostaining of laminin at 120 h (Fig. 4d): Identification of deposits of BM laminin (in dot shape) was much reduced. We speculate that laminin, a major component of the BM network, by providing affinity binding sites for Ca^{2+} could modify the electrical properties of CMs through control of the extracellular Ca^{2+} and its potential transmembrane exchange as originally proposed by Frank and colleagues.[10,12–21]

Supplementary Material

Refer to Web version on PubMed Central for supplementary material.

Acknowledgments

The authors want to thank Dr. Terri Bruce from Clemson Light Imaging Facility for the help with confocal microscopy. This work was partially supported by National Institutes of Health (P20RR021949 and 5R01 HL085847); National Science Foundation (MRI CBET-0923311 and SC EPSCoR RII EPS-0903795 through SC GEAR program).

REFERENCES

1. Baudino TA, Carver W, Giles W, Borg TK. Cardiac fibroblasts: friend or foe? Am. J. Physiol. Heart Circ. Physiol. 2006; 291:H1015–H1026. [PubMed: 16617141]
2. Bers DM, Shannon TR. Calcium movements inside the sarcoplasmic reticulum of cardiac myocytes. J. Mol. Cell Cardiol. 2013; 58:59–66. [PubMed: 23321551]
3. Borg TK, Gay RE, Johnson LD. Changes in the distribution of fibronectin and collagen during development of the neonatal rat heart. Coll. Relat. Res. 1982; 2:211–218. [PubMed: 6759014]
4. Bray MA, Adams WJ, Geisse NA, Feinberg AW, Sheehy SP, Parker KK. Nuclear morphology and deformation in engineered cardiac myocytes and tissues. Biomaterials. 2010; 31:5143–5150. [PubMed: 20382423]
5. Brette F, Salle L, Orchard CH. Quantification of calcium entry at the T-tubules and surface membrane in rat ventricular myocytes. Biophys. J. 2006; 90:381–389. [PubMed: 16214862]
6. Brette F, Orchard C. T-tubule function in mammalian cardiac myocytes. Circ. Res. 2003; 92:1182–1192. [PubMed: 12805236]
7. Bursac N, Parker KK, Iravanian S, Tung L. Cardiomyocyte cultures with controlled macroscopic anisotropy: a model for functional electrophysiological studies of cardiac muscle. Circ. Res. 2002; 91:e45–e54. [PubMed: 12480825]
8. Dworak BJ, Wheeler BC. Novel MEA platform with PDMS microtunnels enables the detection of action potential propagation from isolated axons in culture. Lab. Chip. 2009; 9:404–410. [PubMed: 19156289]
9. Farhadian F, Contard F, Sabri A, Samuel JL, Rappaport L. Fibronectin and basement membrane in cardiovascular organogenesis and disease pathogenesis. Cardiovasc. Res. 1996; 32:433–442. [PubMed: 8881506]
10. Frank JS, Brady AJ, Farnsworth S, Mottino G. Ultrastructure and function of isolated myocytes after calcium depletion and repletion. Am. J. Physiol. 1986; 250:H265–H275. [PubMed: 3946627]
11. Frank JS, Langer GA. The myocardial interstitium: its structure and its role in ionic exchange. J. Cell Biol. 1974; 60:586–601. [PubMed: 4824287]
12. Frank JS, Langer GA, Nudd LM, Seraydarian K. The myocardial cell surface, its histochemistry, and the effect of sialic acid and calcium removal on its structure and cellular ionic exchange. Circ. Res. 1977; 41:702–714. [PubMed: 71221]
13. Gambaro G, Cavazzana AO, Luzi P, Piccoli A, Borsatti A, Crepaldi G, et al. Glycosaminoglycans prevent morphological renal alterations and albuminuria in diabetic rats. Kidney Int. 1992; 42:285–291. [PubMed: 1328749]
14. Gonzalez AM, Buscaglia M, Ong M, Baird A. Distribution of basic fibroblast growth factor in the 18-day rat fetus: localization in the basement membranes of diverse tissues. J. Cell Biol. 1990; 110:753–765. [PubMed: 1689733]
15. Hallmann R, Horn N, Selg M, Wendler O, Pausch F, Sorokin LM. Expression and function of laminins in the embryonic and mature vasculature. Physiol. Rev. 2005; 85:979–1000. [PubMed: 15987800]
16. Kuhl U, Ocalan M, Timpl R, Mayne R, Hay E, von der Mark K. Role of muscle fibroblasts in the deposition of type-IV collagen in the basal lamina of myotubes. Differentiation. 1984; 28:164–172. [PubMed: 6396135]
17. LaFramboise WA, Scalise D, Stoodley P, Graner SR, Guthrie RD, Magovern JA, et al. Cardiac fibroblasts influence cardiomyocyte phenotype in vitro. Am. J. Physiol. Cell Physiol. 2007; 292:C1799–C1808. [PubMed: 17229813]
18. Langer GA, Frank JS. Lanthanum in heart cell culture. Effect on calcium exchange correlated with its localization. J. Cell Biol. 1972; 54:441–455. [PubMed: 5044754]
19. Langer GA, Frank JS, Nudd LM, Seraydarian K. Sialic acid: effect of removal on calcium exchangeability of cultured heart cells. Science. 1976; 193:1013–1015. [PubMed: 948758]
20. Langer GA, Frank JS, Philipson KD. Ultra-structure and calcium exchange of the sarcolemma, sarcoplasmic reticulum and mitochondria of the myocardium. Pharmacol. Ther. 1982; 16:331–376. [PubMed: 6291075]

21. Langer GA, Frank JS, Rich TL, Orner FB. Calcium exchange, structure, and function in cultured adult myocardial cells. Am. J. Physiol. 1987; 252:H314–H324. [PubMed: 3812748]
22. Liu H, Shao Y, Qin W, Runyan RB, Xu M, Ma Z, et al. Myosin filament assembly onto myofibrils in live neonatal cardiomyocytes observed by TPEF-SHG microscopy. Cardiovasc. Res. 2012
23. Lundgren E, Gullberg D, Rubin K, Borg TK, Terracio MJ, Terracio L. In vitro studies on adult cardiac myocytes: attachment and biosynthesis of collagen type IV and laminin. J. Cell Physiol. 1988; 136:43–53. [PubMed: 3294238]
24. Ma Z, Liu Q, Liu H, Yang H, Yun JX, Eisenberg C, et al. Laser-patterned stem-cell bridges in a cardiac muscle model for on-chip electrical conductivity analyses. Lab. Chip. 2012; 12:566–573. [PubMed: 22170399]
25. McGarvey ML, Baron-Van Evercooren A, Kleinman HK, Dubois-Dalcq M. Synthesis and effects of basement membrane components in cultured rat Schwann cells. Dev. Biol. 1984; 105:18–28. [PubMed: 6381174]
26. Miner JH. Organogenesis of the kidney glomerulus: focus on the glomerular basement membrane. Organogenesis. 2011; 7:75–82. [PubMed: 21519194]
27. Miner JH. The glomerular basement membrane. Exp. Cell Res. 2012; 318:973–978.
28. Nitkin RM, Rothschild TC. Agrin-induced reorganization of extracellular matrix components on cultured myotubes: relationship to AChR aggregation. J. Cell Biol. 1990; 111:1161–1170. [PubMed: 2167896]
29. Paralkar VM, Vukicevic S, Reddi AH. Transforming growth factor beta type 1 binds to collagen IV of basement membrane matrix: implications for development. Dev. Biol. 1991; 143:303–308. [PubMed: 1991553]
30. Ross RS, Borg TK. Integrins and the myocardium. Circ. Res. 2001; 88:1112–1119. [PubMed: 11397776]
31. Sanborn WG, Langer GA. Specific uncoupling of excitation and contraction in mammalian cardiac tissue by lanthanum. J. Gen. Physiol. 1970; 56:191–217. [PubMed: 5433467]
32. Simpson DG, Terracio L, Terracio M, Price RL, Turner DC, Borg TK. Modulation of cardiac myocyte phenotype in vitro by the composition and orientation of the extracellular matrix. J. Cell Physiol. 1994; 161:89–105. [PubMed: 7929612]
33. Thyberg J, Hultgardh-Nilsson A. Fibronectin and the basement membrane components laminin and collagen type IV influence the phenotypic properties of subcultured rat aortic smooth muscle cells differently. Cell Tissue Res. 1994; 276:263–271. [PubMed: 8020062]
34. Vernier RL, Klein DJ, Sisson SP, Mahan JD, Oegema TR, Brown DM. Heparan sulfate–rich anionic sites in the human glomerular basement membrane. Decreased concentration in congenital nephrotic syndrome. N. Engl. J. Med. 1983; 309:1001–1009. [PubMed: 6225948]
35. Vukicevic S, Kleinman HK, Luyten FP, Roberts AB, Roche NS, Reddi AH. Identification of multiple active growth factors in basement membrane Matrigel suggests caution in interpretation of cellular activity related to extracellular matrix components. Exp. Cell Res. 1992; 202:1–8. [PubMed: 1511725]
36. Wang J, Hoshijima M, Lam J, Zhou Z, Jokiel A, Dalton ND, et al. Cardiomyopathy associated with microcirculation dysfunction in laminin alpha4 chain-deficient mice. J. Biol. Chem. 2006; 281:213–220. [PubMed: 16204254]
37. Yurchenco PD. Basement membranes: cell scaffoldings and signaling platforms. Cold Spring Harb. Perspect. Biol. 3:2011.
38. Yurchenco PD, Cheng YS. Self-assembly and calcium-binding sites in laminin. A three-arm interaction model. J. Biol. Chem. 1993; 268:17286–17299. [PubMed: 8349613]
39. Zhang P, Su J, Mende U. Cross talk between cardiac myocytes and fibroblasts: from multiscale investigative approaches to mechanisms and functional consequences. Am. J. Physiol-Heart C. 2012; 303:H1385–H1396.

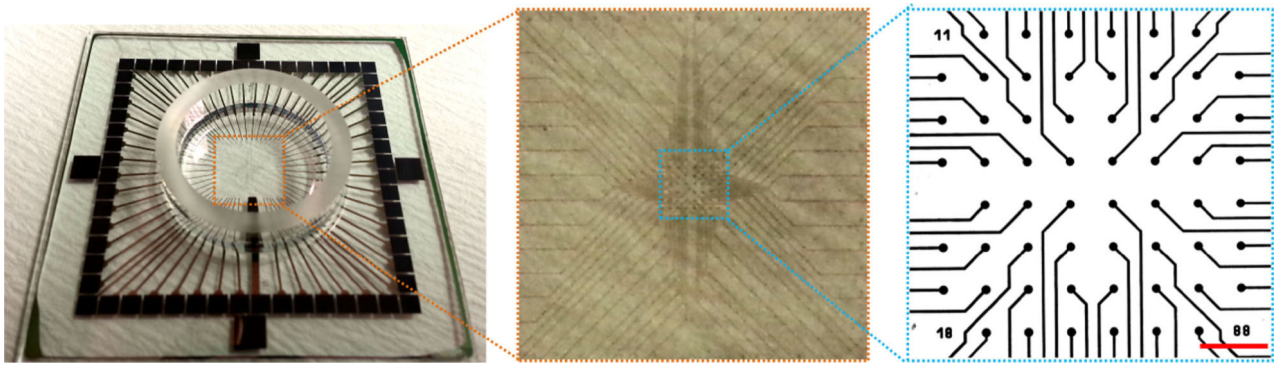

FIGURE 1.

View of MEA chip and distribution of 60 microelectrodes on the chip. Scale bar: 300 μm.

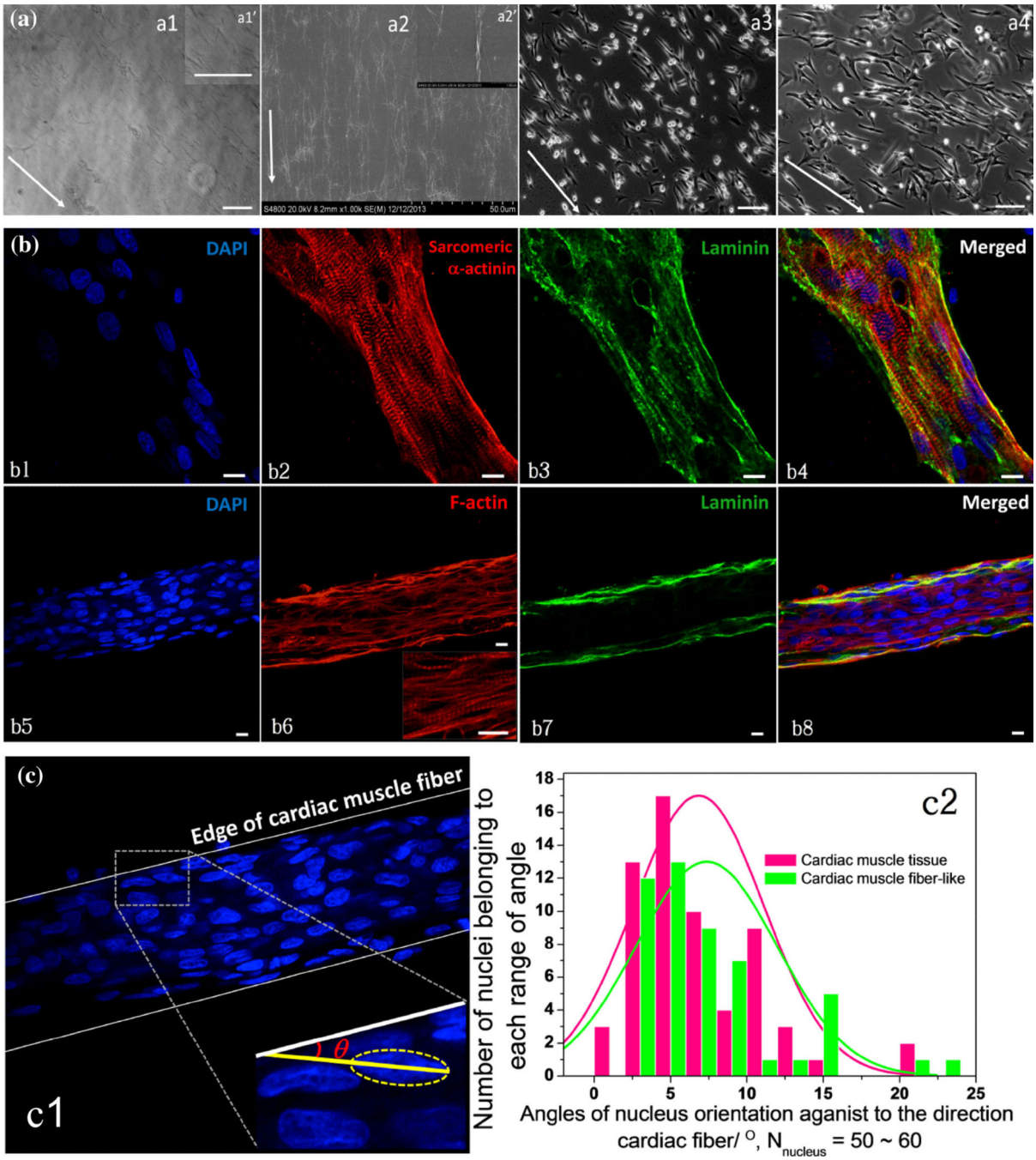

FIGURE 2.

(a) a1: Morphologies of ACG coating on a glass coverslip; a1′: Upper-right box: enlarged image of aligned collagen I fibrils. a2: Collagen fibrils formed on ACG-coated coverslip imaged by SEM; a2′: Upper-right box: enlarged image of aligned collagen I fibrils imaged by SEM. a3 and a4: NCMs cultured on ACG at 24 and 48 h, arrows indicate orientations of ACG, scale bars: 100 μm. (b) Confocal images of immunocytostaining of nucleus (DAPI in blue, b1 and b5), sarcomeric α-actinin (red, b2), *F*-actin (red, b6), and laminin (green, b3 and b7) of NCMs cultured on ACG at 192 h, scale bars: 10 μm. (c) Evaluation of angle θ c1) of nucleus orientation to the edge of cardiac muscle fiber-like structure comparing it to cardiac muscle tissue, 50–60 nuclei were evaluated in each group, their distributions of θ are shown in the histogram of c2, $p = 0.24 > 0.05$.

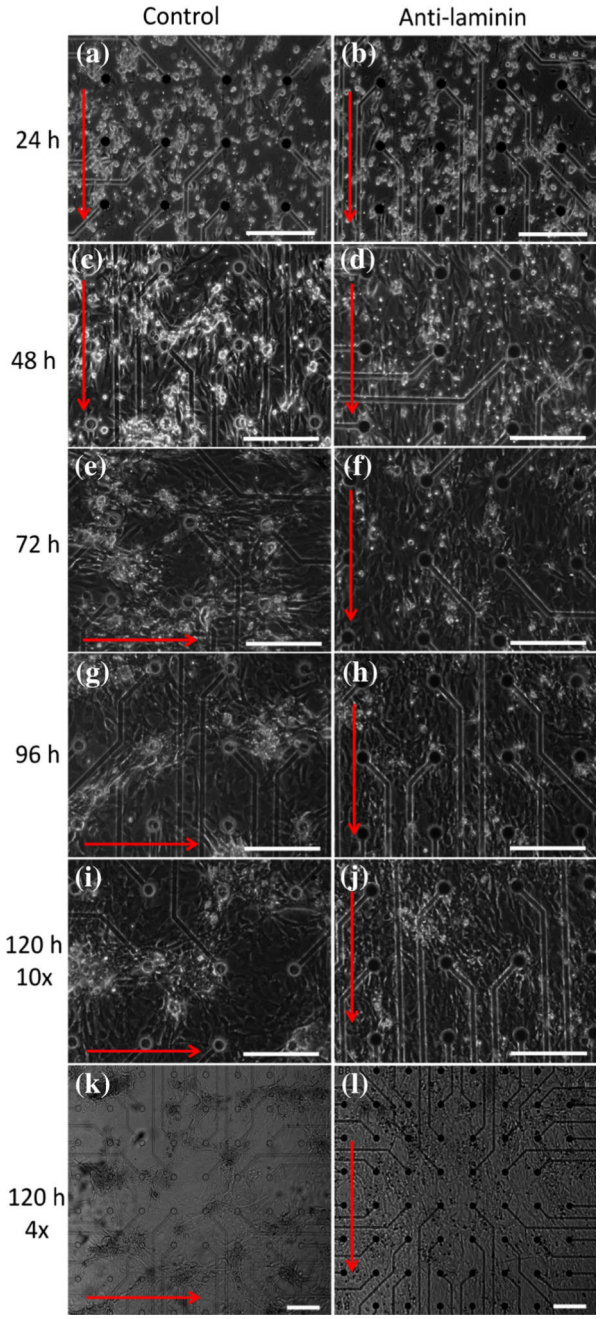

FIGURE 3.

Morphologies of NCMs growing on the ACG-coated MEA chip in control and anti-laminin groups from 24 to 120 h. (a, c, e, g, i and k) Control group cultured at 24, 48, 72, 96, 120 (10×) and 120 (4×) h, respectively. (b, d, f, h, j and l) Anti-laminin group cultured at 24, 48, 72, 96, 120 (10×) and 120 (4×) h, respectively. Red arrows indicate the directions of collagen fibrils. Scale bars: 200 μm.

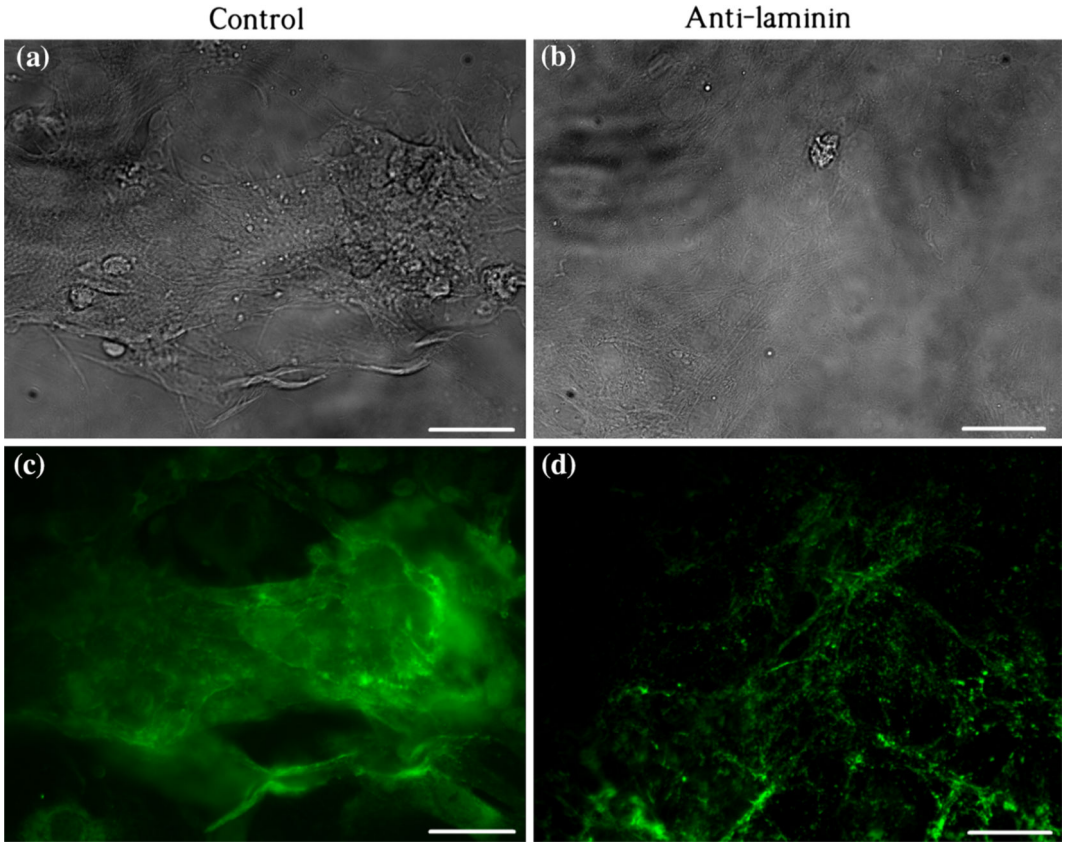

FIGURE 4.

Immuocytostaining of laminin on NCMs being cultured at 120 h. (a and c) Phase and fluorescent images in the control group, respectively. (b and d) Phase and fluorescent images in the anti-laminin group, respectively. Scale bars: 20 μm.

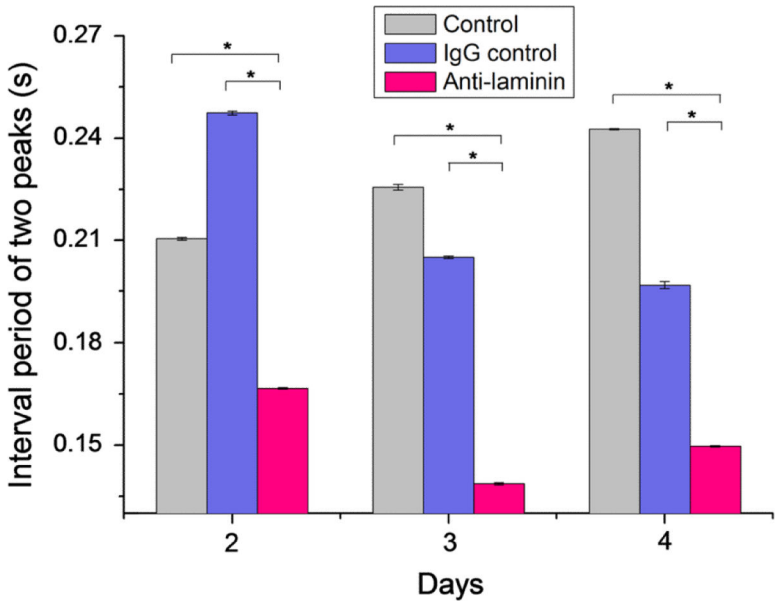

FIGURE 5.

Interval periods of two adjacent upper peaks of three groups: Control, IgG control, and anti-laminin at Days 2, 3, and 4. $N = 12$, $*p < 0.01$.

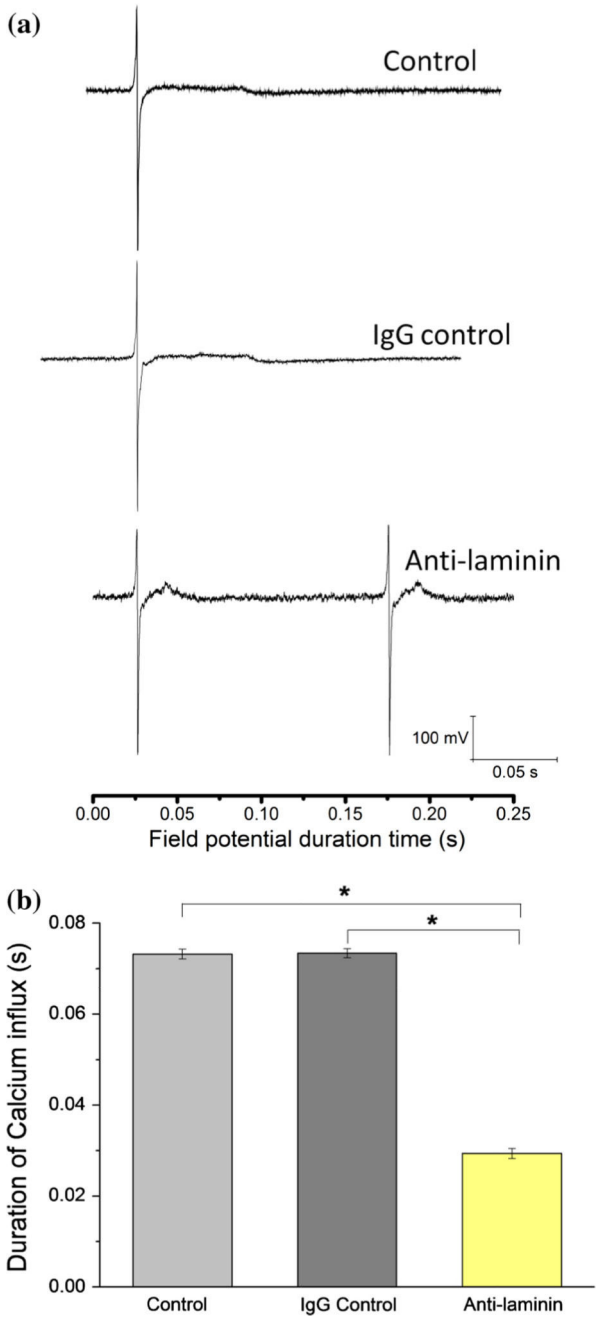

FIGURE 6.

(a) Patterns of field potential of NCMs cultured on MEA chips at Day 4 of three groups: Laminin—rabbit-anti-rat IgG laminin antibody added into culture medium; CD105—rabbit-anti-rat IgG CD105 added into culture medium as IgG control; control—only culture medium without addition of antibodies. Plateau is highlighted as calcium ion influx. (b) Durations of calcium influx of three groups: Laminin, CD105, and control at day 4. * $P < 0.01$, $n = 12$.

TABLE 1

Sum of interval periods of two peaks and durations of plateau of field potential measured by MEA chip in three groups on Day 4: Control, *I*g control and anti-laminin.

Time/s	Control	*I*g control	Anti-laminin
Interval period of two peaks[a]	0.2430 ± 0.0002	0.1968 ± 0.0011	0.1497 ± 0.0003
Duration of plateau of calcium flux[a]	0.0732 ± 0.0011	0.0734 ± 0.0010	0.0294 ± 0.0011

[a]The data are the results measured on the 12 microelectrodes in each group ($N = 12$).